JOURNAL OF Materials CHEMISTRY

Fast ion conduction in the Li-analogues of Nasicon, $Li_{1+x}[(Ta_{1-x}Ge_x)Al](PO_4)_3$

C. J. Leo, G. V. Subba Rao and B. V. R. Chowdari*

Department of Physics, National University of Singapore, Singapore 119260. E-mail: phychowd@nus.edu.sg; Fax: 65-777-6126

Received 27th November 2001, Accepted 8th March 2002
First published as an Advance Article on the web 10th April 2002

Fast lithium ion conducting Nasicon compounds, $Li_{1+x}[(Ta_{1-x}Ge_x)Al](PO_4)_3$, $x = 0$–1.0 have been synthesized, characterized by X-ray diffraction and X-ray photoelectron spectroscopy (XPS) and their ionic conductivities were determined as a function of temperature (T) and frequency (f) by the impedance technique. The hexagonal lattice parameters and cell volume showed a systematic change with the germanium dopant, x. The XPS Li(1s) spectra show two peaks with binding energies (BEs) of 55.0 and 55.9 eV for all the Ge-doped compounds, due to lithium ion occupation in the Type I and II lattice sites. The measured σ_{ionic} at 60 °C varies from 2.1–5.5 × 10^{-5} S cm^{-1} for x in the range 0.4–0.8 and E_a and log σ_o go through a broad minimum and maximum respectively. From an analysis of σ_{ionic} *vs.* f at various T, the f-independent $\sigma_{ionic(dc)}$, the hopping frequency (f_p) of the mobile lithium ions and the exponent n of the ac dispersive regime were determined. The values of the activation energies of the ac and dc conductivity and that of the hopping process were found to be the same, implying that the mobile ion concentration is T-independent. Also, the low-frequency dispersion due to the electrode polarization appears to correlate with that of the f-independent dc conductivity.

Introduction

The search for fast lithium (Li) ion conducting solid electrolytes in realizing all-solid-state high energy density Li-batteries is ongoing and has intensified during the last decade. These batteries use Li-metal or a Li-alloy as the anode. Li-analogues of Nasicon represent a promising series of compounds due to their structural framework and uniformly high Li-ion conductivities encountered at room and elevated temperatures. These compounds continue to receive attention as prospective solid electrolytes and have been reviewed in the literature.[1–3] Sodium zirconium phosphate, $NaZr_2(PO_4)_3$ (NZP) is the parent compound of Nasicon and has a hexagonal crystal structure. The structure consists of ZrO_6 octahedra and PO_4 tetrahedra, which share all their vertices to form a 3D-network with interconnected channels. The Na-ions are located in these channels and can occupy two distinct sites, called Type I and II. In NZP, only Type I sites are filled and Type II sites are empty, whereas in Nasicon ($Na_3Zr_2PSi_2O_{12}$) some of the Type II sites are also filled. Chemical substitution at the Na- and Zr-sites is possible and a large number and wide variety of isostructural Li-compounds of the type, $Li(M_2^{4+})(PO_4)_3$, M = Ti, Zr, Hf, Ge, Sn;[1–3] $Li_{1+x}(M_{2-x}^{4+},M'^{3+}_x)(PO_4)_3$, M = Ti, Zr, Hf, Ge, Sn; M′ = Al, Ga, In;[1,2] $Li_{1-x}(M_{2-x}^{4+}, M'^{5+}_x)(PO_4)_3$, M = Nb, Ta; M′ = Al, Cr, Fe;[1,2] $Li(M^{5+},M'^{3+})(PO_4)_3$, M = Nb, Ta; M′ = Al, Cr, Fe[3,4] and $Li_2(M^{4+},M'^{3+})(PO_4)_3$, M = Ti, Zr, Hf; M′ = Cr, Fe, In[5] have been synthesized and studied for Li-ion conduction behaviour. Ionic conductivities (σ_{ionic}) of the order of 10^{-5} S cm^{-1} at 25 °C and as high as 1 × 10^{-2} S cm^{-1} at 350 °C, and activation energies (E_a) for conduction in the range 0.3–0.6 eV have been reported. For some compositions, it has been possible to synthesize glass-ceramics where the ceramic (crystalline) phase possesses the Li-Nasicon structure and high σ_{ionic} at 25 °C have been realized.[6–9] Glass-ceramics have some advantages over sintered polycrystalline ceramics for practical applications. Recently, fabrication and testing of all-solid-state Li-batteries using $Li(Ti_2^{4+})(PO_4)_3$ as the solid electrolyte have been reported.[10]

Efforts have been made to correlate the σ_{ionic} and E_a with the crystallographic unit cell volume (V) in the series of compounds $Li(M_{2-x}^{4+},M'^{4+}_x)(PO_4)_3$, M ≠ M′ = Ti, Hf, Ge.[1,2] It was noted that the phase with M = M′ = Ti, possesses the highest σ_{ionic} at 25 °C, the lowest E_a and a V of 1310 Å^3 and possibly represents an optimum tunnel (bottle neck) size for Li-ion motion in the lattice. With M′ = Ge or Hf, it was possible to vary the V as a function of x. The E_a was found to remain low (0.28–0.30 eV) in a narrow range of V (1290–1330 Å^3) and increased or decreased appreciably when V was greater or smaller than the above value. Thangadurai *et al.*[4] in their studies on the system $Li(M^{5+},M'^{3+})(PO_4)_3$, M = Nb, Ta; M′ = Al, Cr, Fe, found high σ_{ionic} at 30 °C and low E_a (0.47 eV, range 30–250 °C) in the compound $Li(Ta^{5+},Al^{3+})(PO_4)_3$ and noted that its unit cell volume of 1315 Å^3 falls within the optimum range of V mentioned above for the Li-Nasicon phase. The latter compound could be a prospective candidate for all-solid-state Li-batteries since Ta- and Al-oxides and -phosphates are inert to chemical attack (reduction) by Li-metal or -alloy unlike the Ti^{4+}-compounds. It will be of interest to extend the ionic conductivity studies to the germanium (Ge)-doped $Li(Ta,Al)(PO_4)_3$ where the Type II sites are also filled by Li, and to examine whether the empirical correlation between the V and E_a observed earlier[1,2,4] still holds good in this case. We note that Ge-oxide and -phosphate are also inert to attack by Li-metal. Here we report the synthesis, characterization and σ_{ionic} studies on compounds $Li_{1+x}[(Ta_{1-x}^{5+},Ge_x^{4+})Al](PO_4)_3$, $0 < x < 1$.

Experimental

The series of compounds $Li_{1+x}[(Ta_{1-x}Ge_x)Al](PO_4)_3$ where $x = 0$ to 1 were prepared by high temperature solid-state reaction. Stoichiometric amounts of reagent grade chemicals namely lithium carbonate (Li_2CO_3), aluminium hydroxide ($Al(OH)_3$), tantalum oxide (Ta_2O_5), germanium oxide (GeO_2) and ammonium dihydrogen phosphate ($(NH_4)H_2PO_4$) were used as the starting materials. The precursors were thoroughly mixed in an agate mortar grinder and heated initially at 600 °C in alumina crucibles for 6 hours. The initial heating is done to

 DOI: 10.1039/b110863h

This journal is © The Royal Society of Chemistry 2002

decompose Li_2CO_3 and $(NH_4)H_2PO_4$ with the emission of ammonia, carbon dioxide gases and water vapour. The mixture was then cooled, reground, pressed into pellets and reheated in the alumina crucible at 950 °C for 24 h and cooled slowly to room temperature at the rate of 5 °C min^{-1}. For the compounds with $x > 0.7$, heating to a temperature of 950 °C was found to result in slight melting and hence those compositions were heated at 900 °C for 24 h. The pellets were then ground to fine powder for characterization.

The compounds were characterized by powder X-ray diffraction (XRD) (Philips X'PRT-MPD system; Cu-Kα radiation; $2\theta = 10$–$70°$). X-Ray photoelectron spectroscopy (XPS) measurements were done using a VG ESCALAB MK II spectrometer; Mg-Kα radiation. The samples were vacuum dried and loaded for XPS measurements by dusting powder onto a polymeric-based adhesive tape. The spectra were fitted using the standard XPSPEAK software and internal corrections of the binding energy were done using the difference between the adventitious C(1s) peak and the standard C(1s) value of 284.6 eV. All curve fittings were done using 80% Lorentzian and 20% Gaussian curves. For ionic conductivity measurements, thin pellets (0.5–1.5 mm thick and 1.3 cm diameter) were made from the fine powder using poly(vinyl alcohol) (PVA) as the binder. The pellets were then heated by slowly raising the temperature to 600 °C, at the rate of 0.5 °C min^{-1} and maintained at that temperature for 10 hours. This is to eliminate the binder from the samples. The temperature was then increased to 800 °C at the rate of 2 °C min^{-1}, maintained for 24 h and then slowly cooled to room temperature at the rate of 2 °C min^{-1}. Dense pellets with a smooth surface were thus obtained. The pellets were then gold coated on either side using a JEOL, JFC-1100 ion sputtering unit. Measurements were carried out using a Solartron 1470 battery test unit in the frequency range from 10 Hz to 1 MHz, with the temperature ranging from 25 to 120 °C.

Results and discussion

XRD

The synthesized compounds, $Li_{1+x}[(Ta_{1-x}^{5+},Ge_x^{4+})Al](PO_4)_3$, $0 \leqslant x \leqslant 1$, are white, crystalline and stable in air. The XRD patterns indicate the formation of a Li- Nasicon phase with a hexagonal structure, Fig. 1. Traces of impurities, mainly attributable to the compound $AlPO_4$ were seen in all the phases. An additional impurity due to GeO_2 was also seen for the phases with $x = 0.9$ and 1.0. Under the synthesis conditions employed, the solubility limit for Ge appears to be $x \leqslant 0.9$. For the compositions with $x \geqslant 0.6$, splitting of the (*hkl*) line near

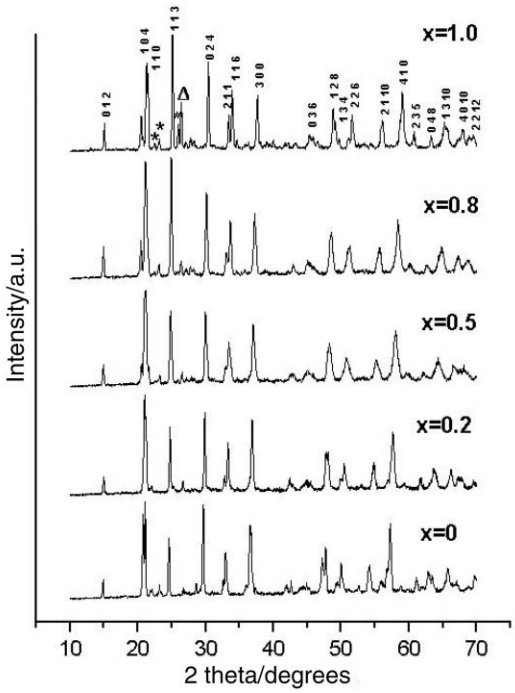

Fig. 1 Powder X-ray diffraction patterns of compounds $Li_{1+x}[(Ta_{1-x}Ge_x)Al](PO_4)_3$. Values of x and Miller indices (*hkl*) are indicated. Impurity peaks: (* = Li_3PO_4; # = GeO_2; Δ = $AlPO_4$).

the doublet (104,110) peak (around $2\theta = 21°$) was seen, indicative of monoclinic distortion of the hexagonal lattice. However, the line assigned to (116) was not found to split for the above values of x showing that the distortion is small. Monoclinic distortion of the hexagonal structure of Li-Nasicon phases is known to occur either as a function of decreasing temperature or due to the multiple chemical substitution at the M,M′ sites which may lead to the Li-ion occupancy both at Type I and II sites.[1–3,11] Since the distortion is small, XRD patterns of the presently synthesized compounds have been indexed as the hexagonal structure. The least square fitted a and c lattice parameters and the unit cell volume (V) for the phases with $0 \leqslant x \leqslant 1$ are listed in Table 1. Our a and c values for $Li(Ta^{5+},Al^{3+})(PO_4)_3$ ($x = 0.0$) are slightly different from those reported by Thangadurai *et al.*[4] for this composition, in that our a is smaller and c is larger by 0.034 and 0.409 Å respectively. Thus, our value of V is larger (1340 $Å^3$) than their value by 1.9%. The a value increases and c decreases for $x = 0.1$. For higher values of x including $x = 1.0$, the a decreases systematically with the exception of $x = 0.8$, for

Table 1 Lattice parameters, unit cell volume, conductivity and XPS Li(1s) binding energy of the compounds $Li_{1+x}[(Ta_{1-x}Ge_x)Al](PO_4)_3$

Composition, x in $Li_{1+x}[(Ta_{1-x}Ge_x)Al](PO_4)_3$	Hexagonal lattice parameters and unit cell volume			Conductivity		XPS Li (1s)			
						Binding energy (BE)/eV (±0.1)		Relative peak area	
	a/Å (±0.005)	c/Å (±0.01)	V/$Å^3$ (±5)	$\sigma_{60\,°C} \times 10^{-6}$/ S cm^{-1}	$\sigma_{120\,°C} \times 10^{-5}$/ S cm^{-1}	Type I	Type II	Type I	Type II
0	8.518	21.32	1340	0.25	0.43	55.4	—	—	—
0.1	8.525	21.16	1332	0.25	0.35	55.0	55.9	0.77	0.23
0.2	8.517	21.16	1329	0.96	1.03	55.0	56.0	0.61	0.39
0.3	8.487	21.08	1315	2.11	1.94	55.1	55.8	0.61	0.39
0.4	8.463	21.01	1303	19.88	15.18	55.1	56.0	0.66	0.34
0.5	8.422	20.97	1288	24.39	21.25	55.1	56.0	0.62	0.38
0.6	8.415	20.83	1277	54.78	46.54	55.1	56.1	0.60	0.40
0.7	8.362	20.79	1259	39.56	33.46	55.0	55.9	0.58	0.42
0.8	8.366	20.69	1254	31.92	25.85	55.0	55.7	0.56	0.44
0.9	8.308	20.54	1228	11.68	9.00	54.9	55.9	0.54	0.46
1.0	8.283	20.58	1223	3.08	2.82	54.9	55.9	0.54	0.46

which the value is almost same as that for $x = 0.7$(Table 1). For $x = 0.1$ and 0.2, the c value remains constant and for the range, $x = 0.2$–0.9, there is a continuous decrease. It increases slightly for $x = 1.0$. However, we note that compounds with $x = 0.9$ and 1.0 are not single-phase and contain GeO_2 impurity. In the range $x = 0.2$–1.0, V decreases in a linear fashion with a small deviation at $x = 0.9$ (Table 1). The variation of a, c and V *vs.* x can be understood from ionic radii considerations, since Ta^{5+}($r = 0.64$ Å)[12] is being substituted by the smaller size Ge^{4+}($r = 0.53$ Å) in $Li_{1+x}[(Ta_{1-x}^{5+}, Ge_x^{4+})Al](PO_4)_3$. Similar behavior has been observed in the series of compounds $Li_{1+x}[(Ti_{2-x}^{4+}, Al_x^{3+})](PO_4)_3$[8] and $Li_{1+x}Ti_{2-x}^{4+}(P_{3-x}^{5+}, Si_x^{4+})O_{12}$.[7]

XPS

Though it is a surface technique, the XPS spectra and the binding energies (BE) of the elements present in Nasicon and other crystalline oxide systems can give information on the site-occupancy of the ions and their coordination with respect to the oxygen ions.[9,13] Since in the present series of compounds, the Li ions are expected to occupy Type I and/or Type II sites depending on the value of x, we may expect subtle differences in the Li(1s) spectra, and the BEs. In addition, when two different sites are occupied by Li ions, the area under the peaks can give an approximate estimate of relative site-occupancies. Wide scan spectra of all the compositions ($x = 0$–1.0) were obtained in the range 0–1100 eV. High-resolution spectra of select elements in the desired range were then taken. The Li(1s) peaks of select compositions are shown in Fig. 2 and the BEs are listed in Table 1. The low signal-to-noise ratio of the Li spectra is due to the low scattering factor of lithium. For $x = 0$, the peak looks symmetrical and hence was fitted with a single curve and the BE was found to be 55.4 eV. This is assigned to the Li ions at the Type I site and agrees with the value of 55.0 eV reported for Li(1s) in the glass ceramic system, Li_2O–Al_2O_3–MO_2–P_2O_5 (M = Ti and Ge).[9] With the substitution of germanium at the octahedral sites (x), a considerable shift of (decrease by 0.4 eV) the Li(1s) peaks was noticed. In addition, the peak broadens and becomes slightly asymmetric. The raw spectra were deconvoluted into two peaks, with BEs at ~55 eV and ~56 eV. Though the presence of the second peak is inconspicuous for the lower values of x, at higher compositions ($x \geqslant 0.6$), the presence cannot be ruled out. The increase in area of the second peak indicates an increase in the number of Li-ion occupations of the site with increasing x. This second Li(1s) peak with higher BE of 55.9 ± 0.2 eV is attributed to the Li-ions at the Type-II sites. A higher BE signifies higher ionicity of the Li–O bond and hence a greater mobility and increased contribution to the ionic conductivity.

A decrease in the BE of Li(1s) by 0.4 eV when x is increased from 0 to 0.1 is a clear indication of the change in the environment around Li-ions occupying Type I sites as a result of Ge doping. The invariance of the BE at 55.0 ± 0.1 eV and at 55.9 ± 0.2 eV for all values of x (0.1–1.0; Table 1), indicates that the environment around the Li ions at the Type I and II sites remains unchanged. Also, the relative increase in the corresponding peak area of the Type II sites (Table 1) with the increase in x, is an indication of the increase in the number of Li-ions at this site and hence the ionic conductivity.

Ionic conductivity

In the present series of compounds, all metal ions are in their maximum possible valency states and thus have negligible electronic conductivity. Since they possess the Nasicon structure, we do expect high values of σ_{ionic} both as a function of x and temperature. These can be correlated to draw significant conclusions. We have obtained σ_{ionic} from the impedance (Cole–Cole) plots for various compositions in the range 25–120 °C. The data are given in Table 1 and the impedance plots for select compositions (x) at 60 °C are shown in Fig. 3. For the lower contents of germanium $x = 0.1$–0.3, two semicircles are seen overlapping, but for $x > 0.3$, only one semicircle is seen. The small semicircle observed for $x \leqslant 0.3$ at a higher frequency (10^5 Hz) can be attributed to the impedance due to the bulk of the grains of the material. The large semicircle in the frequency range of 10^3 Hz is due to the grain boundary impedance. From Fig. 3, a decrease in the total resistance of the compound with increasing germanium content (up to $x = 0.6$) is clearly seen. The intercept of the large semicircle on the x-axis (Z') is taken as the total resistance (R). σ_{ionic} was then calculated for a given x from R, the thickness (l)

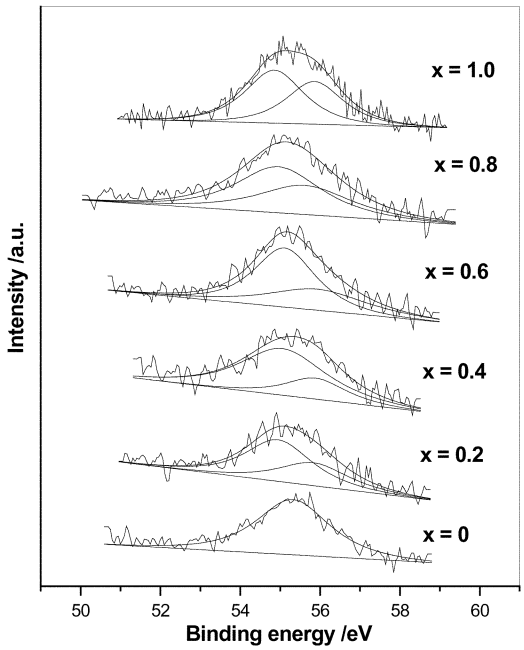

Fig. 2 The Li(1s) XPS spectra of the compound $Li_{1+x}[(Ta_{1-x}Ge_x)Al](PO_4)_3$ for select compositions (x).

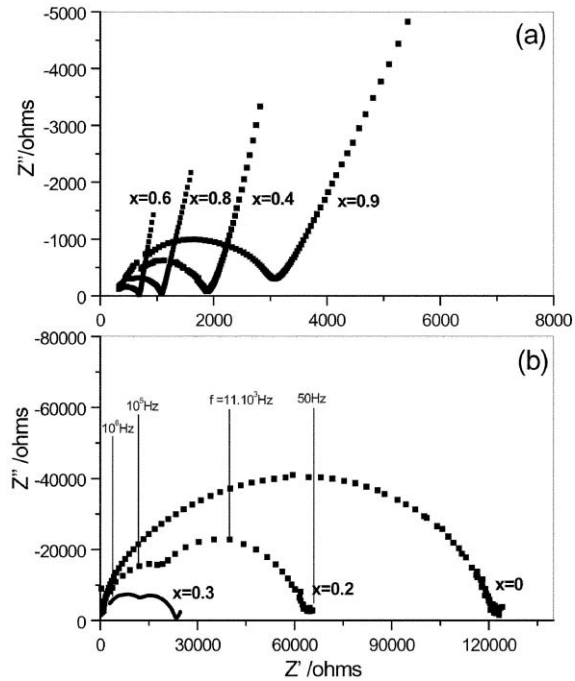

Fig. 3 Impedance (Cole–Cole) plots for select compositions x in $Li_{1+x}[(Ta_{1-x}Ge_x)Al](PO_4)_3$. Temperature, $T = 60$ °C.

and area (A) of the pellet: $\sigma = (1/R)(l/A)$. The conductivity data were fitted to the Arrhenius equation,

$$\sigma T = \sigma_o \exp(-E_a/k_B T) \quad (1)$$

where E_a is the activation energy, σ_o the pre-exponential factor and k_B the Boltzmann's constant. The σ_{ionic} values at 60 °C and 120 °C as a function of x are given in Table 1. As can be seen, the maximum conductivity was obtained for the composition with $x = 0.6$ ($V = 1277$ Å^3; $\sigma_{60\ °C} = 54.8 \times 10^{-6}$ S cm^{-1}) which is more than two orders of magnitude greater than the undoped compound ($x = 0$) ($\sigma_{60\ °C} = 0.25 \times 10^{-6}$ S cm^{-1}). Our σ_{ionic} values for $x = 0$ lie in the range observed for the same composition by Thangadurai *et al.*[4] The σ_{ionic} of the optimized composition in our present system is comparable to the Li-σ_{ionic} of the titanium based Li-Nasicon system $Li_{1.3}(Al_{0.3}Ti_{1.7})(PO_4)_3$[1] ($\sigma_{30\ °C} = 7 \times 10^{-4}$ S cm^{-1}), the perovskite phase $(La_{0.55}Li_{0.36})TiO_3$ system[3] ($\sigma_{30\ °C} \approx 1.5 \times 10^{-3}$ S cm^{-1}) and the Na-σ_{ionic} of the Nasicon system $Na_{1+x}Zr_2P_{3-x}Si_xO_{12}$[2] ($\sigma_{30\ °C} \approx 10^{-3}$ S cm^{-1}).

Fig. 4 shows the temperature dependence of the conductivity (Arrhenius plots) of the series of compounds $Li_{1+x}[(Ta_{1-x}Ge_x)Al](PO_4)_3$ in the range 60–120 °C. The composition dependence of conductivity is well illustrated in the figure, where the Arrhenius plot gets shifted with the change in x. The curve of $x = 0.6$ with the maximum σ_{ionic} seems to have the optimum germanium content and the compositions with greater and lower values of x show a decreasing conductivity trend. The values E_a and $\log_{10} \sigma_o$ are plotted against x in Fig. 5. Our value of E_a for $x = 0$ is higher by 0.1 eV than that reported by Thangadurai *et al.*[4] The E_a decreases with increasing x, more drastically till x reaches 0.4 and goes through a broad minimum in the range $x = 0.5$–0.8, Fig. 5. On the other hand, $\log_{10} \sigma_o$ goes through a minimum for $x = 0.2$–0.3 and then through a maximum at around $x = 0.6$. The pre-exponential factor which signifies the number of mobile lithium ion charge carriers shows high values for $x = 0.4$–0.6, since for these compositions the number of vacant and filled Type II interstitial sites are well balanced. This is reflected in the low E_a and high σ_{ionic} observed for these compositions.

As mentioned earlier, Li-analogues of Nasicon, $Li(M_{2-x}^{4+}, M'_x{}^{4+})(PO_4)_3$, M ≠ M′ = Ti, Hf, Ge were found to exhibit high σ_{ionic} and low E_a when V is in the range, 1290–1330 Å^3.[12] In the present system, $\sigma_{60\ °C}$ varies from 2.0–5.5 × 10^{-5} S.cm^{-1} for x in the range 0.4–0.8 (Table 1). Also, for the same range of x, E_a and $\log \sigma_o$ go through a broad minimum and maximum respectively and the respective V values span the range, 1254–1303 Å^3 (Fig. 5 and Table 1). Thus, in the present (Ta–Ge–Al) series, higher conductivity is observed in the range of V, which is slightly lower than the range reported in the literature for the (Ti–Ge; Ti–Hf) series.[1,2] However, the above empirical correlation must be viewed with some reservation since in the present series, $Li_{1+x}[(Ta_{1-x}^{5+},Ge_x^{4+})Al](PO_4)_3$, $0 < x < 1$, the Li ions occupy both Type I and partly Type II sites (for $x > 0$), the measured σ_{ionic} includes inter-grain contributions and the obtained E_a values are higher than that encountered in the pure Ti-compound, $Li(Ti_2^{4+})(PO_4)_3$, *viz.*, 0.30 eV.[1,2] Also, the M^{5+} cation is now partly occupying the octahedral sites in the present series instead of the M^{4+} ions reported in the literature. The presence of the higher positively charged cation in the lattice may be influencing the Li^+ ion migration and has resulted in a decreased unit cell volume for the optimum lithium ion migration.

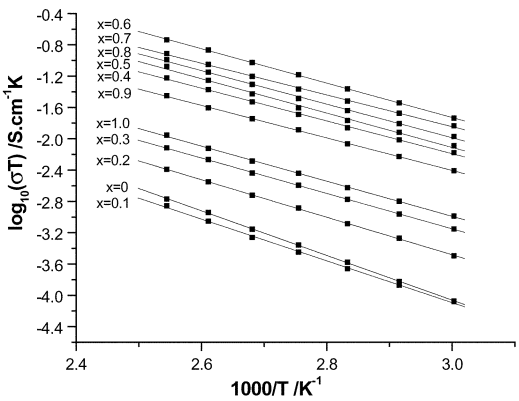

Fig. 4 Arrhenius plots (log (σT) *vs.* 1000/T) of the compounds, $Li_{1+x}[(Ta_{1-x}Ge_x)Al](PO_4)_3$ in the temperature range 60–120 °C.

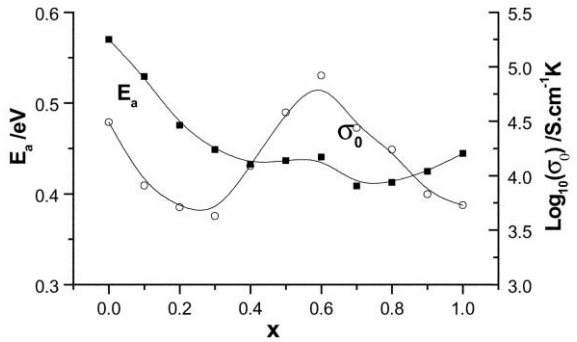

Fig. 5 Variation of the activation energy (E_a) and the pre-exponential factor (σ_o) as a function of x in $Li_{1+x}[(Ta_{1-x}Ge_x)Al](PO_4)_3$.

Frequency dependence of ionic conductivity

Analysis of the frequency dependence of ionic conductivity at various temperatures of the fast ion conductors can give insights into the hopping (jump) frequency of the ions, their T-dependence, extrapolated-dc conductivity and also whether the mobile ion concentration is thermally activated. Such an analysis, both of theoretical and experimental data has been done for a variety of crystalline and glassy solids.[14–19] We have presently measured the σ_{ionic} as a function of the applied frequency (f) at various temperatures for select compositions, $x = 0$, 0.3, 0.6 and 0.9 in $Li_{1+x}[(Ta_{1-x}^{5+},Ge_x^{4+})Al](PO_4)_3$. The data are shown in Fig. 6 as the log–log plots. The shape and evolution of the curves with temperature undergoes significant changes with the different values of x. Three distinct regions in the conductivity spectra are observed for the compounds with $x = 0.6$ and 0.9: (i) the high frequency dispersive region ($f > 10^4$ Hz), (ii) the middle plateau region, which is the

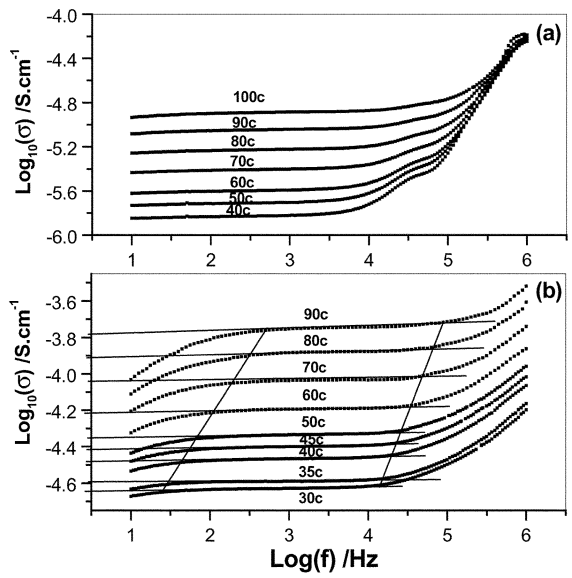

Fig. 6 Log–log plots of σ *vs.* frequency (f) at different temperatures. (a) $x = 0.3$ and (b) $x = 0.6$.

so-called dc regime and (iii) the low frequency dispersive region. The latter is not seen for $x = 0$ and 0.3 at any of the measured temperatures. The first region, which is purely the dispersive component of the ac conductivity together with the middle plateau (frequency independent) region, can be expressed by the generalized power-law equation[14] at a given temperature (T) as,

$$\sigma(f) = \sigma_o' + Af^n \quad (2)$$

where σ_o' is the extrapolated conductivity value of the frequency independent region, A is the ac coefficient and n is the exponent. The cross-over point of the frequency-independent plateau and the high frequency ac dispersive region shifts towards the high frequency values with increasing temperature, Fig. 6. This can be explained by the fact that with the increase in T, the kinetic energy of the ions also increases and hence their vibrational frequency. The onset points of the conductivity dispersion at different temperatures are found to lie on a straight line and for $x = 0.6$, the line was found to be inclined at an angle of around 47 degrees (slopes ≈ 1), Fig. 6b. This implies that $\sigma_o'(T)$ and the onset-frequency $f(T)$ are proportional to each other and both are thermally activated with almost the same energy of activation indicating a general feature of the power law proposed by Jonscher.[15,16]

Since the electrical response is reflected in the characteristics of the dynamics of the hopping ions and assuming that the same mobile charge carrier ions participate in both ac and dc conductivity,[14] eqn. (2) can be modified as

$$\sigma(f) = kf_p + kf_p^{1-n}f^n \quad (3)$$

where f_p is the hopping frequency and k is set equal to $(Ne^2a^2/k_BT)\gamma C(1 - C)$ by comparison with the equation for the dc ionic conductivity:[14]

$$\sigma_{dc} = (2\pi Ne^2a^2/k_BT)\,)\gamma C(1 - C)f_p \quad (4)$$

where C is the mobile ion concentration distributed over N equivalent sites per unit volume, e the electronic charge, a the hopping distance, k_B Boltzmann's constant, T the temperature, γ the correlation factor, and f_p the hopping frequency. Hence, from eqns. (2) and (3), we get $\sigma(f) = 2\sigma_o'$ when $f = f_p$, which allows one to determine the σ_o' and hopping frequency (f_p) from the experimental data. The f_p and the σ_o' values have been obtained from the log (σ) *vs.* log (f) plots for compositions $x = 0$, 0.3, 0.6 and 0.9. Values of f_p range from 0.4–92.5 $\times$ 10^4 Hz depending on T and x. The σ *vs.* f plots at different temperatures in Fig. 6 have been scaled down to merge one over the other using the scaling parameters σ_o' and f_p as adopted by Sidebottom *et al.*[17] This resulted in a single curve with a T-independent exponent, n, suggesting a temperature independent relaxation mechanism. The scaled-curves for the compositions $x = 0.6$ and 0.9 give a value $n = 0.61$ and 0.63 respectively for the temperature range 40–90 °C. For the lower compositions, $x = 0$ and 0.3, the n values were found to vary with T and the average n is $\sim$0.9. The exponent n, which signifies the inter-ionic interactions of the mobile ions[18,19] observed for the compositions with $x > 0.5$ are within the range typical of what had been reported in the literature for various ionic conductors.[20] The reason for the observed high value of n for $x < 0.5$ is presently not known and to be investigated.

Arrhenius-type plots of f_p and σ_o' *vs.* T for select compositions x are shown in Fig. 7. As can be seen the corresponding energies of activation, E_a^{dc} and $E_a^{f_p}$ are almost the same for a given value of x. This result is not surprising, since the slope of the line joining the points of onset frequency in Fig. 6b has a slope around unity. Also, the macroscopic activation energies (E_a) obtained from the log (σT) *vs.* $1/T$ plots in Fig. 4 have

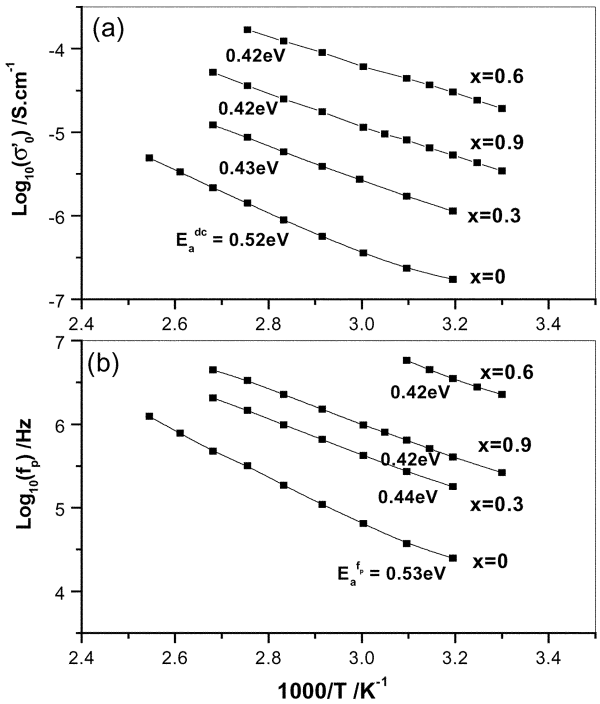

Fig. 7 Arrhenius-type plots: (a) $\log_{10}$ (σ_o') and (b) $\log_{10}$ (f_p) *vs.* 1000/T, in the temperature range (60–120 °C) for compounds $Li_{1+x}[(Ta_{1-x}Ge_x)Al](PO_4)_3$, $x = 0$, 0.3, 0.6 and 0.9. Energies of activation are given.

almost the same values as those of the $E_a^{f_p}$ and E_a^{dc} for a given x (Fig. 7). Hence, it is evident that the T-dependence of the ac and dc conductivity and the hopping frequency are similar and indicates that the carrier concentration is T-independent in this series of compounds and is solely determined by the initial chosen value of x.

The low frequency dispersion observed for compositions $x = 0.6$ and 0.9 at various temperatures is due to the electrode polarization as a result of the accumulation of mobile ions at the interface. The development of the space charge accumulation is more effective at lower frequencies.[21] Therefore, the total σ_{ionic} of the compound decreases as frequency decreases at a given temperature. The conductivity drop can be seen in Fig. 6 for the frequency values below the middle plateau (dc) frequency regime. The dispersion is steeper and also the onset-point of the low frequency dispersion shifts to a higher frequency value with increasing temperature. This is due to the fact that at higher temperatures the mobility of the ions is higher resulting in faster and more accumulation of ions and hence a corresponding drop in total conductivity. As observed in the case of high-frequency dispersion, the low frequency onset-points at different temperatures lie in a straight line inclined at an angle 38° (Fig. 6b). Hence, the low frequency dispersion in conductivity, $\Delta\sigma$ ($=\sigma_o' - \sigma_{total}$), at a given T is found to depend on the magnitude of the frequency-independent dc conductivity (σ_o'). This is shown in Fig. 8, where $\Delta\sigma$ *vs.* σ_o' follows a straight-line for two select compositions ($x = 0.6$ and 0.9). Thus, in the present series of compounds, frequency dependence of σ_{ionic} at various temperatures has provided insight into the microscopic Li-ion motion in the Nasicon lattice.

Conclusions

Fast ion conducting lithium analogues of Nasicon, $Li_{1+x}[(Ta_{1-x}^{5+},Ge_x^{4+})Al](PO_4)_3$, $x = 0$–1.0 have been synthesized, characterized by XRD and XPS and their ionic conductivities have been obtained as a function of temperature (25–120 °C) and applied ac frequency (10^1–10^6 Hz) from the impedance measurements. The hexagonal a and c parameters were found

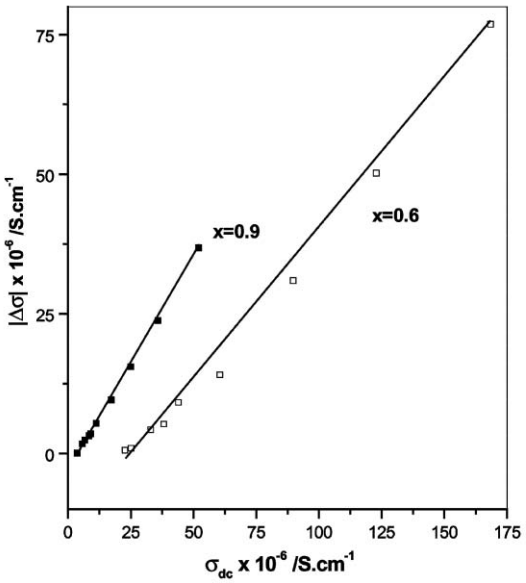

Fig. 8 Plot of low-frequency dispersion in conductivity ($|\Delta\sigma| = \sigma'_o - \sigma_{total}$) *vs.* frequency-independent dc conductivity (σ'_o) for $x = 0.6$ and $x = 0.9$ in $Li^{1+x}[(Ta_{1-x}Ge_x)Al](PO_4)_3$.

to decrease with x in the range 0.1–1.0, whereas the unit cell volume (V) showed a continuous decrease for all x. The XPS Li(1s) spectra of the different compositions ($x > 0.1$), showed two peaks which are assigned to the lithium ion occupation in the Type I and II sites in the Nasicon structure and which are separated by a BE of around 1.0 eV. The Li–O bond in the Type II sites seems to be more ionic in nature and hence an enhancement in the conductivity was observed with increasing x up to 0.6. The measured σ_{ionic} (at 60 °C) varies from 2.1–5.5 × 10^{-5} S.cm^{-1} for x in the range 0.4–0.8. Also, in the same range of x, E_a and log σ_o go through a broad minimum and maximum respectively. The respective V values for $x = 0.4$–0.8 span the range, 1254–1303 Å^3. Analysis of the σ_{ionic} *vs.* frequency at various temperatures for select compositions (x) enabled the extraction of $\sigma_{ionic(dc)}$, hopping frequency (f_p)and the values of n, the exponent in the generalized power-law. For $x = 0.6$ and 0.9, $n \approx 0.6$. The f_p varies from 0.4–92.5 × 10^4 Hz depending on the values of x and T. It was found that E_a is almost the same as that of $E_a^{f_p}$ and E_a^{dc} for a given x, implying that the mobile-ion concentration remains the same in the measured range of temperature. The low-frequency dispersion in σ_{ionic} seen for $x = 0.6$ and 0.9 at several temperatures could be correlated to the respective $\sigma_{ionic(dc)}$. The present study shows that the compounds with $x = 0.4$–0.8 exhibit σ_{ionic} comparable to some of the best observed in the Li-analogues of Nasicon ($Li(Al,Ti)(PO_4)_3$), and with the added advantage of stability in contact with Li-metal, these phases are indeed potential candidates as the solid electrolytes in all-solid-state Li-batteries.

Acknowledgement

The authors thank Dr. K. M. Shaju, for useful discussions and to Ms. Y. J. Liu, Surface Science Lab I, for the help in obtaining the XPS data. Thanks are also due to Mr. Karim, for his assistance.

References

1 H. Aono, N. Imanaka and G. Y. Adachi, *Acc. Chem. Res.*, 1994, **27**, 265.
2 G. Y. Adachi, N. Imanaka and H. Aono, *Adv. Mater.*, 1996, **8**, 127.
3 J. Gopalakrishnan, A. K. Shukla and V. Thangadurai, *Curr. Sci.*, 1999, **76**, 1473.
4 V. Thangadurai, A. K. Shukla and J. Gopalakrishnan, *J. Mater. Chem.*, 1999, **9**, 739.
5 M. Sugantha and U. V. Varadaraju, *Solid State Ionics*, 1997, **95**, 201.
6 J. Fu, *Solid State Ionics*, 1997, **104**, 191.
7 J. Fu, *J. Am. Ceram. Soc.*, 1997, **80**, 1901.
8 J. Fu, *J. Mater. Sci.*, 1998, **33**, 1549.
9 B. V. R. Chowdari, G. V. Subba Rao and G. Y. H. Lee, *Solid State Ionics*, 2000, **136–137**, 1067.
10 P. Birke, F. Salam, S. Doring and W. Weppner, *Solid State Ionics*, 1999, **118**, 149.
11 M. Cretin and P. Fabry, *J. Eur. Ceram. Soc.*, 1999, **19**, 2931.
12 R. D. Shannon, *Acta Crystallogr., Sect. A*, 1976, **32**, 751.
13 B. V. R. Chowdari, G. V. Subba Rao and C. J. Leo, *Mater. Res. Bull.*, 2001, **36**, 727.
14 D. P. Almond and A. R. West, *Solid State Ionics*, 1983, **9–10**, 277.
15 A. K. Jonscher, *Nature*, 1977, **267**, 673.
16 K. Funke, *Progr. Solid State Chem.*, 1993, **22**, 111.
17 D. L. Sidebottom, P. F. Green and R. K. Brow, *J. Non-Cryst. Solids*, 1997, **222**, 354.
18 S. R. Elliott, *Solid State Ionics*, 1988, **27**, 131.
19 K. L. Ngai, A. K. Rajagopal and S. Teitler, *J. Chem. Phys.*, 1988, **88**, 5086.
20 D. L. Sidebottom, P. F. Green and R. K. Brow, *J. Non-Cryst. Solids*, 1995, **183**, 151.
21 H. J. Schutt and E. Gerdes, *J. Non-Cryst. Solids*, 1992, **144**, 1.